Nanoscale

Nucleation of hematite nanocrystals revealed by a single nanoseconds laser pulse method

Journal:	*Nanoscale*
Manuscript ID	NR-COM-04-2018-003069.R2
Article Type:	Communication
Date Submitted by the Author:	20-Jun-2018
Complete List of Authors:	Liu, Zhikun; South China University of Technology, Materials Science and Engineering Liu, C. Richard; Purdue University , Industrial Engineering

Nucleation of hematite nanocrystals revealed by a single nanoseconds laser pulse method

Zhikun Liu[1,2*] and C. Richard Liu[1]

Abstract: Full understanding about how nanocrystals nucleate is mainly inhibited by two factors: 1) lack of a comprehensive theoretical framework which can explain and predict the occurrence of nonclassical indirect nucleation pathway, and 2) lack of a high temporal and spatial resolution observation method to study the nucleation process. Here we introduce a single nanoseconds laser pulse method with TEM observation to reveal the nucleation mechanism of hematite nanocrystals. The single pulse experimental design aims at revealing the phenomenon at the earliest stage of the crystallization process. The short nanoseconds heating duration prevents the aging process which might obscure the precise nucleation information for the TEM study. By this method, it is shown that the nucleation pathway of hematite nanocrystals can be tuned by the energy input of the laser pulse. Hematite crystals, amorphous materials or both are nucleated depending on the energy of the first laser pulse. We believe the short laser pulse method is a valuable method to study other nucleation phenomena at nanoscale and will contribute to deepening our understanding about how different material structures form at the very early stage.

The formation of nanomaterials from solution begins with a nucleation process which is critical to the structure and size distribution of the materials.[1] Phenomena outside of the scope of classical nucleation theory, such as formation of dense liquid-like clusters, were recently observed and confirmed.[2] Nucleation from solution can proceed through direct pathway, indirect pathway or coexistence of the both.[3] Thus a new theoretical framework that explains and predicts the occurrence of different nucleation pathway is desirable.[4] However, progress towards a more comprehensive theory has been impeded by technical limitations in probing the nucleation process at the nanoscale and at the relevant time.[5]

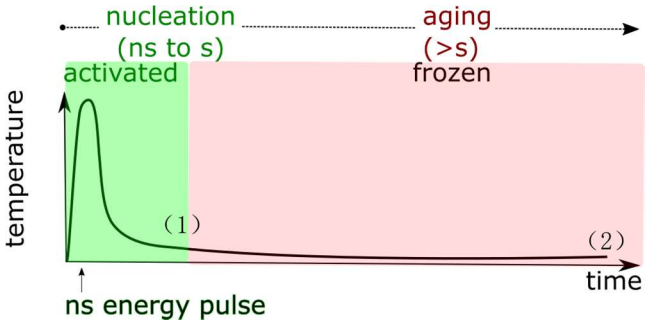

Figure 1. Schematic of temperature response due to a short energy pulse heating

One of the technical difficulties lies in freezing the fast dynamic process of crystallization for detailed investigation. Here we propose a short single energy pulse method. The supersaturation and kinetics for phase transformation were set at sufficient low values. The crystallization was thermally activated only for a short period of time by a single energy pulse. The goal was to partially initiate the nucleation process and inhibit the aging process, such as solid state recrystallization or dissolution-reprecipitation. In this case, study of the system at a later stage, such as stage (2) in Figure 1 was expected to provide important information regarding what happened at the very early stage, such as stage (1) in Figure 1.

Continuous or pulsed laser irradiation have been used to induce nucleation of a variety of materials, including metals,[6–8] oxides,[9–13] potassium chloride,[14,15] and organic molecules.[16,17] In particular, the development of laser-induced photothermal growth method enabled selective integration of heterogeneous nanomaterials with high precision and controllability.[18–22] However, the studies were essentially focused on the crystal yield and final structure. The dynamics of the nucleation process were not investigated quantitatively. Nucleation usually occurs on a small time scale, from nanoseconds to seconds.[23] The aim of the present work is to take advantage of the short time span of a single nanoseconds laser pulse to investigate phenomena at the early stage of crystallization processes. We performed single pulse (about 8 ns heating time) and multiple pulses (maximum 16 μs heating time) experiments to study the nucleation process of iron oxide from solution. Details about the experiment setting are available in the Electronic Supporting Information (ESI). We found that the nucleation pathway of hematite nanocrystals can be controlled by the energy of first laser pulse.

The synthesis of hematite in an acidic solution is typically carried out at a temperature higher than 90 °C.[24] In this work, we set the solution temperature at 25 °C so that no spontaneous nucleation occurred due to a slow kinetic state. A nanoseconds laser pulse (5 ns pulse width, 1064 nm wavelength) was used to induce nucleation of hematite. Molecular dynamics simulations demonstrated that it took about tens of nanoseconds for an iron oxide nanoparticle to complete its nucleation process.[25] 5 ns pulse width laser was chosen to realize the design as shown in Figure 1. In addition, it was designed to limit laser-nuclei interaction which can accelerate order development due to direct heating. The bandgap of Fe_2O_3 is 2.1 eV.[26] Thus laser light with much lower photon energy of 1.2 eV (corresponding to 1064 nm wavelength) was used. The laser light travelled through a thin layer of aqueous solution (4 mm deep). Its energy is absorbed by a copper grid and copper plate assembly and the resulting heat pulse (peak temperature higher than 74°C) activated

[1]Dr. Zhikun Liu, Dr. C. Richard Liu
[1]School of Industrial Engineering and Birck Nanotechnology Center, Purdue University, West Lafayette,IN 47907, USA
[2]*Dr. Zhikun Liu
School of Materials Science and Engineering, South China University of Technology, Guangzhou, 510640, China
Email: liuzhikun@scut.edu.cn

nucleation of iron oxides in the vicinity of the copper material. Particles that adhered to a silicon oxide thin film which was attached to the copper were studied by ex situ TEM imaging with atomic resolution. Previous studies[11,26] have shown evidences, suggesting laser induced formation of iron oxides in electrolyte solution is a photo-thermal process rather than photochemical one or the nonphotochemical laser-induced nucleation (NPLIN)[16] process. More information regarding the design of few seconds under the electron beam. The ease of morphology change suggested the high diffusivity of atoms in the amorphous materials. When the energy of single laser pulse was further reduced to 160 mJ, nanocrystals cannot be found and amorphous particle was the only type of material observable. One amorphous particle is shown in Figure 2G. The particle also had the droplet-like shape. When the energy input level of the single laser pulse was reduced to 150 mJ, even amorphous

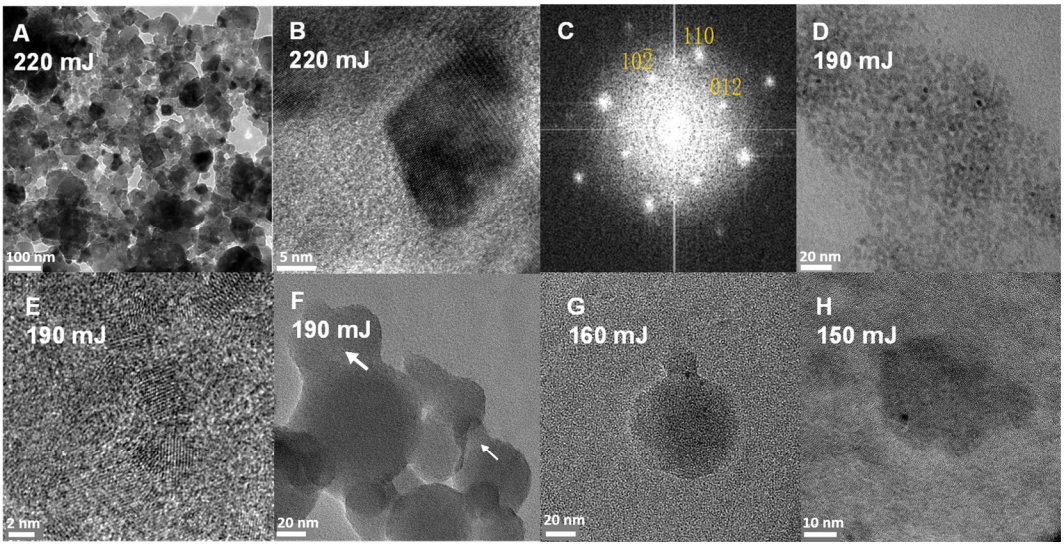

Figure 2. Dependence of nucleus structure on single laser pulse energy. One 220 mJ laser pulse irradiation resulted in formation of hematite crystals as shown in A and B (the fast Fourier transform is shown in C); a mixture of crystalline (D and E) and amorphous particles (F) formed when the pulse energy was 190mJ; one 160 mJ or 150 mJ laser pulse irradiation resulted in only amorphous particle nucleation (G and H respectively).

experiments and discussion upon the laser effect can be found in the ESI.

One Laser Pulse. Different material structures were formed as a result of one laser pulse irradiation at different energy amounts. (The laser energies mentioned in the report refer to the energies of the whole laser beam). When the single pulse energy was as high as 220 mJ, the only observable precipitates were polyhedron single crystals, as shown in Figure 2A. A diamond shape crystal with uniform lattice fringes is shown in Figure 2B. The lattice spacing of 0.36 nm and 0.25 nm can be measured from the image. The fast Fourier transformation of the image (shown in Figure 2C) was same as the diffraction pattern of hematite along the [2-21] zone axis. Spots corresponding to (110), (10-2) and (012) planes of hematite were indexed, indicating the crystals were hematite. When the energy of single pulse was reduced to 190 mJ, two types of materials coexisted. The first type was small nanocrystal. The average size of the nanocrystals was about 4 nm which was significantly smaller than that of crystals precipitated at 220 mJ laser pulse. High resolution TEM image of Figure 2E shows the average lattice spacing of a crystal is 0.27 nm, which corresponds to (014) planes of hematite. The second type of material was large amorphous particle, as shown in Figure 2F. Most of the precipitates were in droplet-like rounded shape. No lattice fringe can be observed on the particles. In addition, the morphology of amorphous particles changed under the electron beam exposure. Adjacent particles fused together and connection necks were formed. White arrows in Figure 2F point to locations where boundaries between separated rounded particles were observable before the fusion. The neck formation usually took a particles became scarce. Figure 2H shows an amorphous particle precipitates under this laser energy. No material of any kind can be found when the single laser pulse energy was lower than 150 mJ. The amorphous particles were not further studied by electron diffraction due to its instability under electron beam. The transformation of amorphous materials to crystalline hematite particles under electron beam exposure is shown in the ESI Figure S2.

Order Development. The nanoseconds pulse method also provided a tool to study the order development within the amorphous nucleus with unprecedented temporal resolution. The pulse repetition rate was as low as 5 Hz and copper plate with a good thermal conductivity were used so that heat accumulation effect can be avoided in the multiple pulses experiment (more discussion can be found in the ESI). Previous report on the forced hydrolysis of Fe (III) solution at pH value lower than 1 showed that hematite was the only observable product and amorphous iron hydroxide was absent. [27] By the high temporal resolution laser pulse method introduced here, evidence is provided that an amorphous intermediate phase exists even at pH value lower than 1. The results are shown in Figure 3. For this series of experiment, energy of laser pulse was kept as constant, 120 mJ and number of pulses was the only changing variable. The time between every pulse is 0.2 seconds. After 10 pulses of laser irradiation, amorphous droplet-like particles can be observed. After 100 pulses of laser irradiation, droplet-like shaped amorphous particle cannot be found anymore. Instead, as shown in Figure 3B, the precipitates were porous amorphous materials. The boundary of the amorphous phase was angular instead of rounded. In addition, high density

of black dots (pointed by a green arrow in Figure 3B) can be observed within the amorphous materials. The appearance of dense region (pointed by a green arrow in Figure 3B) and pore (pointed by a yellow arrow in Figure 3B) within the amorphous precursor suggested density variation in solid phase was activated by laser pulses. Rearrangement of amorphous phases had started after 100 pulses. After 1200 pulses of laser irradiation, the sizes of precipitates were larger, as shown in Figure 3C. The precipitates were still porous in irregular shapes. However, individual crystalline regions began to be observable within the amorphous phase. The crystalline regions were randomly oriented. Figure 3D is a high resolution TEM image showing parallel lattice fringes within the precipitate. The average spacing between the fringes was 0.27 nm, which agreed with the spacing of (014) hematite planes. This indicated that the ordering of atoms or crystallization for stable iron oxide structure had begun after 1200 pulses of laser irradiation. The transformation was more complete after 2000 pulses of laser irradiation, which is shown in Figure 3E and 3F. Higher resolution image of Figure 3F reveals that the precipitation became aggregation of randomly oriented nanocrystals. Lattice fringes are visible on the nanocrystals. The average spacing was 0.22 nm which corresponded to (113) hematite planes. The order development process can be summarized as: amorphous particles (10 pulses) → density variation (100 pulses) → birth of crystalline region (1200 pulses) → randomly oriented hematite nanocrystals (≥2000 pulses). For the whole order development process shown in Figure 2, the accumulated heating duration was only about 16 μs.

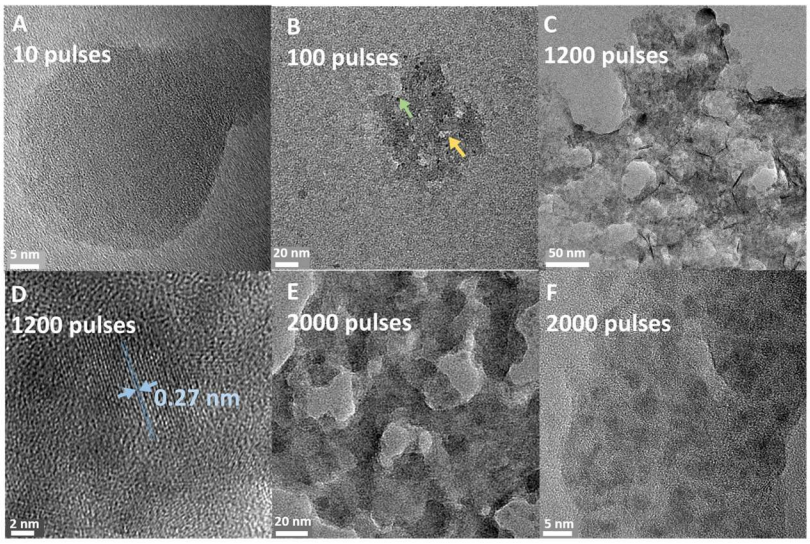

Figure 3. Order development of amorphous nucleus induced by multiple laser pulses at 120 mJ per pulse. After 10 pulses, spherical amorphous structure formed (A), after 100 pulses, porous amorphous structure formed (B), after 1200 pulses, nanocrystals formed within amorphous structure (C and D), after 2000 pulses, massive number of nanocrystals with average size of 3.3 nm formed (E and F).

Nucleation Pathways. The ordering process of iron oxide in Figure 3 followed an indirect nucleation pathway: first nucleation of metastable liquid or solid phase and then slow conversion to a stable crystalline phase. In this study, the materials in the form of amorphous droplet did not show lattice fringes and was dynamic and transient due to the energy input even under an electron beam. Thus we excluded the possibility that amorphous precursor was ferrihydrite[28]. It is likely that the initially formed droplet-like material contained a considerable amount of weak Fe-OH-Fe bonds or trapped water. As shown in Figure S2, the size of amorphous precipitate was reduced significantly under prolonged electron exposure in TEM. The production of leaving water during Fe-OH-Fe bonds condensation can explain the size reduction and the pore formation within amorphous precursor shown in Figure 3B (pointed by yellow arrow). Therefore the evolution process shown in Figure 3 indicated a nonclassical indirect nucleation pathway instead of an aging process of a less stable crystalline phase. The individual pulse method also provided evidences that the formation of hematite nuclei from the pre-existing amorphous materials was the rate limiting step. We measured 47 crystals which were recognizable from the same sample shown in Figure 3F. The average size is 3.3 nm and standard deviation is 0.8 nm, as shown in Figure 4A. Nonclassical indirect pathway offers an effective route to synthesize ultrafine nanocrystals, which are highly desirable in catalyst[29], energy storage[30] and optoelectronics applications[31]. The results explained the formation of ultrafine nanocrystals in multi-pulse laser chemical deposition.[11–13] When diffusion energy barrier inside amorphous precursor is high enough comparable to nucleation energy barrier, ultrafine crystals are formed within the amorphous materials.

The single energy input was designed short enough to prevent the activation of aging process. We estimate the total temperature rise duration to be about 8 ns (See the ESI). The heat pulse did not last long enough for a nucleus to self-assemble, not to mention activating the following aging processes. It suggested the crystal observed in Figure 1A, whose structure is the same as the bulk hematite materials, is the result of a direct single step process. At the laser pulse energy of 220 mJ, the hematite crystals were the only observable precipitates and amorphous particle could not be found. We measured the sizes of 90 crystals induced by a laser pulse at 220 mJ as shown in Figure 2A. The average size was of 51 nm and standard deviation was 13 nm. We used the concepts in classical nucleation theory to estimate the size of critical nucleus, $r^* = \frac{2\gamma}{g_v}$, where γ is surface energy and g_v is Gibbs energy per volume. The size of critical nucleus of hematite in this

solution system was 36 nm (A relatively large size of critical nucleus is correlated to the low supersaturation of electrolyte in order to prevent spontaneous crystallization). As could be seen from Figure 4A, most of the hematite crystals were larger than the estimated critical size and the crystals that were significantly smaller than 36 nm were not observable (crystals smaller than 25 nm). The observations can be explained by the classical nucleation theory: nuclei will grow spontaneously when they are larger than the critical size and become more and more unstable as they get smaller than the critical size.

nucleation theory based on concepts of mechanics.[35] The results from this pulse laser experiment suggested the central role of interactive forces in the new nucleation theory.

In conclusion, nanoseconds laser pulse experiment revealed the nucleation process of iron oxide from solution. Crystal or amorphous material or both nucleated initially, depending on the first laser pulse energy. The result from this experiment design provided insight about nucleation mechanism of hematite nanocrystals in electrolyte solution, indicating the pathway can be tuned by the first energy pulse. The findings, suggested the

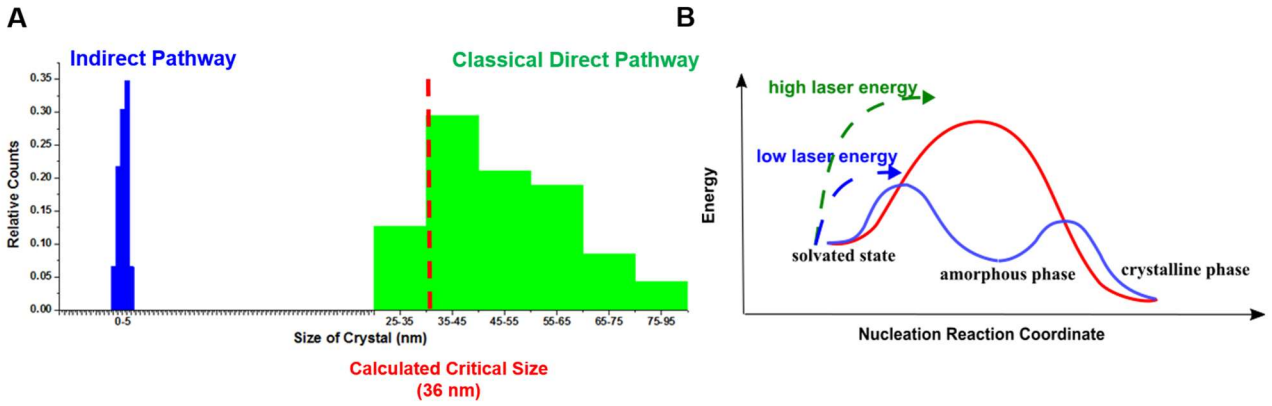

Figure 4. (A) shows dependence of the crystal size on the nucleation pathway. By 220 mJ laser pulse irradiation (1 pulse), hematite nucleated through direct pathway and the average crystal size is 51 nm. By 120 mJ laser pulse irradiation (2000 pulses), hematite nucleated through indirect pathway and the average crystal size is 3.3 nm. (B) summarizes the relationship of Fe_2O_3 nucleation pathways and the energy of first laser pulse.

During the Fe_2O_3 crystallization from electrolyte solution, bonds with different strength may form. [24] Oxo bridges, which have π covalent bonds character produce strong attractive forces than those produced by hydroxo bridges. At acidic condition, the activation energies for oxo bridges formation are only a few kJ/mol.[32] We estimated the peak temperature and the corresponding Boltzmann thermal energies by different energy inputs and the time it took for the temperature rise to dissipate (see the ESI for calculation method and discussion of the results). As could be seen in Table 1, the peak temperatures were 389K and 348K by the energy inputs of 220 mJ and 120 mJ, which corresponded to Boltzmann thermal energies of 3.2 kJ/mol and 2.9 kJ/mol respectively. The laser energies provided thermal energies to activate the formation of chemical bonds of different strength. Colloidal modeling, by varying the frequency of an external electronic field, demonstrated nucleation through classical direct pathway occurred when attractive forces between particles were strong and nucleation through indirect pathway happened when the attractive forces were weak.[34] The modeling result also revealed that crystalline structure and amorphous structure coexisted, at different stages of the nucleation process, when the forces were medium. The mechanism based on strength of the interactive forces is used to explain the experimental phenomenon reported here. High energy input resulted in stronger bonds (*e.g.* oxo bridges) and, according to observations, the occurrence of direct nucleation pathway; whereas low energy input lead to larger amount of weaker bonds (*e.g.* hydroxo bridges) and the occurrence of indirect nucleation pathway. Overcoming shortcomings of the classical nucleation theory including capillary approximation and equilibrium state assumptions, Lutsko developed a new decisive role of interactive force in a more comprehensive nucleation theory. We believe the short laser pulse method is applicable to studying nucleation phenomena of not just hematite, but also other materials. It will contribute to more thorough and quantitative understanding of how different materials form at the beginning.

Energy Input （mJ）	Peak Temperature (K)	Boltzmann Thermal Energy (kJ/mol)
220	389	3.2
190	376	3.1
160	364	3.0
150	360	3.0
120	348	2.9

Table 1. Calculated peak temperatures and Boltzmann thermal energies by different laser energy inputs

Acknowledgement
Authors would like to acknowledge partial financial support from the National Science Foundation under NSF Award Number 1663214.

Electronic Supporting Information Detailed experimental procedure are provided.

Keywords nucleation pathways• crystal sizes• laser• single pulse• iron oxide.

References:

[1] a S. Myerson, B. L. Trout, *Science (80-.).* **2013**, *341*, 855–856.

[2] J. J. De Yoreo, N. A. J. M. Sommerdijk, P. M. Dove, in *New Perspect. Miner. Nucleation Growth*, Springer International Publishing, Cham, **2017**, pp. 1–24.

[3] M. H. Nielsen, S. Aloni, J. J. De Yoreo, *Science (80-.)*. **2014**, *345*, 1158–1162.

[4] J. Baumgartner, A. Dey, P. H. H. Bomans, C. Le Coadou, P. Fratzl, N. a J. M. Sommerdijk, D. Faivre, *Nat. Mater.* **2013**, *12*, 310–4.

[5] M. H. Nielsen, J. J. De Yoreo, in *New Perspect. Miner. Nucleation Growth*, Springer International Publishing, Cham, **2017**, pp. 353–374.

[6] L. Nánai, I. Hevesi, F. V. Bunkin, B. S. Luk'yanchuk, M. R. Brook, G. A. Shafeev, D. A. Jelski, Z. C. Wu, T. F. George, *Appl. Phys. Lett.* **1989**, *54*, 736–738.

[7] V. A. Kochemirovsky, L. G. Menchikov, S. V Safonov, M. D. Bal'makov, I. I. Tumkin, Y. S. Tver'yanovich, *Russ. Chem. Rev.* **2011**, *80*, 869–882.

[8] A. Lachish-Zalait, D. Zbaida, E. Klein, M. Elbaum, *Adv. Funct. Mater.* **2001**, *11*, 218–223.

[9] Z. Liu, C. R. Liu, *Proc. Inst. Mech. Eng. Part N J. Nanoeng. Nanosyst.* **2013**, *228*, 66–72.

[10] C. Fauteux, R. Longtin, J. Pegna, D. Therriault, *Inorg. Chem.* **2007**, *46*, 11036–47.

[11] Z. Liu, C. Richard Liu, *J. Micro Nano-Manufacturing* **2014**, *2*, 011007.

[12] Z. Liu, Z. Cao, B. Deng, Y. Wang, J. Shao, P. Kumar, C. R. Liu, B. Wei, G. J. Cheng, *Nanoscale* **2014**, *6*, 5853–8.

[13] Z. Liu, C. Richard Liu, *Manuf. Lett.* **2013**, *1*, 42–45.

[14] A. J. Alexander, P. J. Camp, *Cryst. Growth Des.* **2009**, *9*, 958–963.

[15] C. Duffus, P. J. Camp, A. J. Alexander, *J. Am. Chem. Soc.* **2009**, *131*, 11676–7.

[16] B. A. Garetz, J. E. Aber, N. L. Goddard, R. G. Young, A. S. Myerson, *Phys. Rev. Lett.* **1996**, *77*, 3475–3476.

[17] I. S. Lee, J. M. B. Evans, D. Erdemir, A. Y. Lee, B. A. Garetz, A. S. Myerson, *Cryst. Growth Des.* **2008**, *8*, 4255–4261.

[18] H. Lee, W. Manorotkul, J. Lee, J. Kwon, Y. D. Suh, D. Paeng, C. P. Grigoropoulos, S. Han, S. Hong, J. Yeo, et al., *ACS Nano* **2017**, *11*, 12311–12317.

[19] S. Hong, H. Lee, J. Yeo, S. H. Ko, *Nano Today* **2016**, *11*, 547–564.

[20] J. Bin In, H.-J. Kwon, D. Lee, S. H. Ko, C. P. Grigoropoulos, *Small* **2014**, *10*, 741–9.

[21] J. Yeo, S. Hong, G. Kim, H. Lee, Y. D. Suh, I. Park, C. P. Grigoropoulos, S. H. Ko, *ACS Nano* **2015**, *9*, 6059–68.

[22] J. Yeo, S. Hong, M. Wanit, H. W. Kang, D. Lee, C. P. Grigoropoulos, H. J. Sung, S. H. Ko, *Adv. Funct. Mater.* **2013**, *23*, 3316–3323.

[23] G. C. Sosso, J. Chen, S. J. Cox, M. Fitzner, P. Pedevilla, A. Zen, A. Michaelides, *Chem. Rev.* **2016**, *116*, 7078–7116.

[24] J.-P. Jolivet, E. Tronc, C. Chanéac, *Comptes Rendus Geosci.* **2006**, *338*, 488–497.

[25] H. Zhang, G. A. Waychunas, J. F. Banfield, *J. Phys. Chem. B* **2015**, *119*, 10630–42.

[26] J. Yeo, S. Hong, W. Manorotkul, Y. D. Suh, J. Lee, J. Kwon, S. H. Ko, *J. Phys. Chem. C* **2014**, *118*, 15448–15454.

[27] J. H. A. Van Der Woude, P. Verhees, P. L. De Bruyn, *Colloids and Surfaces* **1983**, *8*, 79–92.

[28] D. E. Janney, *Clays Clay Miner.* **2000**, *48*, 111–119.

[29] N. D. Loh, S. Sen, M. Bosman, S. F. Tan, J. Zhong, C. A. Nijhuis, P. Král, P. Matsudaira, U. Mirsaidov, *Nat. Chem.* **2016**, DOI 10.1038/nchem.2618.

[30] C. Kim, M. Noh, M. Choi, J. Cho, B. Park, *Chem. Mater.* **2005**, *17*, 3297–3301.

[31] N. T. K. Thanh, N. Maclean, S. Mahiddine, *Chem. Rev.* **2014**, *114*, 7610–30.

[32] J.-P. Jolivet, M. Henry, J. Livage, *Metal Oxide Chemistry and Synthesis: From Solution to Solid State*, Wiley, **2000**.

[33] J.-P. Jolivet, C. Chanéac, E. Tronc, *Chem. Commun.* **2004**, *0*, 477–483.

[34] T. H. Zhang, X. Y. Liu, *Angew. Chemie - Int. Ed.* **2009**, *48*, 1308–1312.

[35] J. F. Lutsko, in *New Perspect. Miner. Nucleation Growth*, Springer International Publishing, Cham, **2017**, pp. 25–41.

TOC Graphic

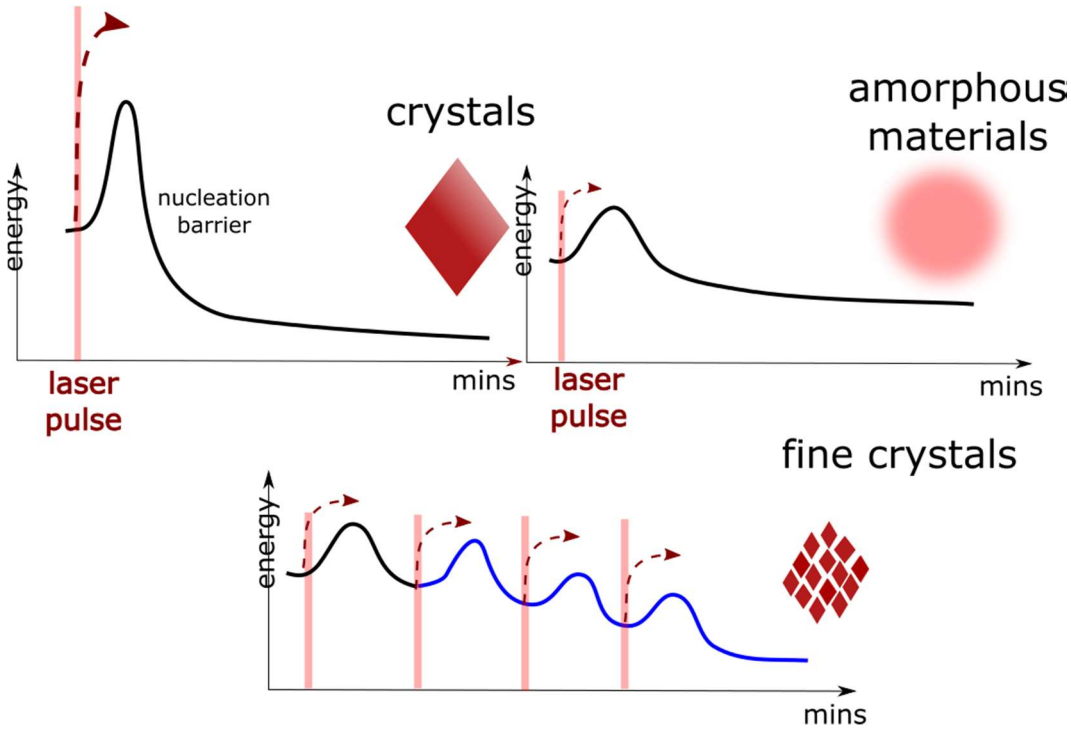
crystals
amorphous materials
energy
nucleation barrier
laser pulse
mins
energy
laser pulse
mins
fine crystals
energy
mins